FRACTAL GEOMETRY AND MIXING TRANSITION IN TURBULENT MIXING LAYER

Mamoru Tanahashi, Yifei Wang, Takeharu Fujisawa,
Makoto Sato, Kazuya Chinda, Toshio Miyauchi
Department of Mechanical and Aerospace Engineering,
Tokyo Institute of Technology
2-12-1 Ookayama, Meguro-ku, Tokyo 152-8850, Japan
mtanahas@mes.titech.ac.jp, wang@navier.mes.titech.ac.jp,
tfujisaw@navier.mes.titech.ac.jp, msato@navier.mes.titech.ac.jp,
kachinda@navier.mes.titech.ac.jp, tmiyauch@mes.titech.ac.jp

ABSTRACT

Direct numerical simulations (DNSs) of turbulent mixing layer with non-reactive and reactive scalar transports have been conducted to investigate the mixing transition mechanism and fractal geometry of scalar surfaces in turbulence. DNS of non-reactive scalar up to $Re_{\omega,0} = 1900$ with moderate Schmidt number (Sc) show that fractal dimension of scalar surfaces in the fully-developed turbulent state is independent to Reynolds number and coincides with the theoretical expectation of Mandelbrot (1975) (≈ 2.5). The inner cutoff is 8 times Kolmogorov length both in the transitional and fully-developed state, and coincides with the most expected diameter of coherent fine scale eddy in turbulence. The mixing transition is characterized by the drastic increase of difference between the outer and inner cutoffs ($Re_\lambda \approx 100$). DNS of reactive scalars show that fractal dimension decreases to $2.40 \sim 2.45$ due to the chemical reaction. The inner cutoff is not affected by the chemical reaction and agrees with that of non-reactive scalars with moderate Sc number. To investigate Schmidt number effects, DNS of non-reactive scalar up to $Sc = 6.0$ has been conducted for moderate Reynolds number. For high Sc, two fractal dimensions can be defined. The first fractal dimension coincides with that of moderate Sc, whereas the second one shows larger values around 2.7. The inner cutoff of the second fractal reaches to about 8 times of Batchelor length scale for high Sc.

INTRODUCTION

The mixing transition in turbulent free shear flows is very important phenomenon in many engineering applications such as chemical process and combustion. This phenomenon can be observed after the turbulence transition of the flow field and enhances scalar mixing significantly (Konrad, 1974; Dimotakis, 2000). However, detailed mechanism of the mixing transition has not been clarified yet. In our previous studies on fine scale structure of turbulence (Tanahashi et al., 1997; 2001; 2004), the existence of universal fine scale structure (coherent fine scale structure), which is independent on Reynolds number and type of flow field, have been revealed. The diameter and the maximum azimuthal velocity of coherent fine scale eddies can be scaled by Kolmogorov length (η) and Kolmogorov velocity (u_k), respectively. Except for near-wall turbulence (Tanahashi et al., 2004), the most expected diameter and maximum azimuthal velocity are 8η and $1.2u_k$. It should be noted that the azimuthal velocity of intense fine scale eddies reaches to $3 \sim 4u'_{rms}$ and are closely related to the intermittency of energy dissipation rate. Since the coherent fine scale structure is a dissipative structure of turbulence and the smallest vortical structure, they would have very important roles on the mixing of heat and mass in turbulence.

In turbulent combustion research, fractal geometry of flame surfaces is very important because the area of flame surface is frequently represented by the ratio of the inner to outer cutoff scale raised to the $2 - D$ power (Gouldin et al., 1989) where D is fractal dimension of the flame surface. The fractal dimension and the inner cutoff of the flame surface has been investigated by many experimental studies (Yoshida et al., 1994; Smallwood et al., 1995; Gülder et al., 2000). However, Gülder et al. (2000) and Gülder and Smallwood (1995) have suggested that the fractal dimension and inner cutoff strongly depend on the measurement and do not agree with expressions proposed by many studies (Peters, 1986; Gouldin, 1987; Gülder, 1990; Poinsot et al., 1990). Therefore, detailed information about the inner cutoff and fractal dimension are necessary to construct the high accuracy turbulent combustion model.

In this study, direct numerical simulations (DNS) of turbulent mixing layer with non-reactive and reactive scalar transports have been conducted to investigate the mixing transition mechanism and fractal geometry of scalar surface in turbulence. The effects of Reynolds number, chemical reaction and Schmidt number are discussed by applying fractal analyses for scalar surfaces obtained from DNS.

DIRECT NUMERICAL SIMULATION OF TURBULENT MIXING LAYER

DNS of temporally developing turbulent mixing layer with different Reynolds number, reaction rate and Schmidt number were conducted by solving following continuity equation, incompressible Navier-Stokes equations and mass conservation equations;

$$\nabla \cdot \boldsymbol{u} = 0, \tag{1}$$

$$\frac{\partial \boldsymbol{u}}{\partial t} + \boldsymbol{\omega} \times \boldsymbol{u} = -\nabla P + \frac{1}{Re_{\omega,0}} \nabla^2 \boldsymbol{u}, \tag{2}$$

$$\frac{\partial Y_A}{\partial t} + \boldsymbol{u} \cdot \nabla Y_A = \frac{1}{ReSc} \nabla^2 Y_A - RcY_A Y_B, \tag{3}$$

$$\frac{\partial Y_B}{\partial t} + \boldsymbol{u} \cdot \nabla Y_B = \frac{1}{ReSc} \nabla^2 Y_B - RcY_A Y_B, \tag{4}$$

where $\boldsymbol{u}$, $\boldsymbol{\omega}$, P and Y_i denote velocity vector, vorticity vector, total pressure ($P = p + \boldsymbol{u}\boldsymbol{u}/2$) and mass fraction of species i, respectively. These equations are non-dimensionalized by

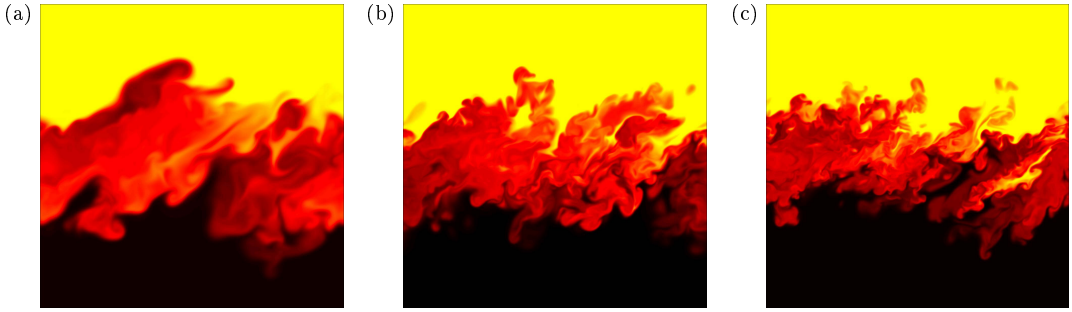

Figure 1: Distributions of scalar mass fraction in fully-developed turbulent state for $Rc = 0$ and $Sc = 0.6$. (a):$Re_{\omega,0} = 500$, (b):$Re_{\omega,0} = 1300$ and (c):$Re_{\omega,0} = 1900$.

Table 1: Numerical parameters for DNS of temporally-developing turbulent mixing layer with non-reactive passive scalar($Sc = 0.6$, $Rc = 0$).

Run ID	$Re_{\omega,0}$	$N_x \times N_y \times N_z$	Re_λ
TMLPS1	500	$216 \times 325 \times 144$	74.6
TMLPS2	900	$324 \times 487 \times 216$	104.2
TMLPS3	1300	$384 \times 577 \times 256$	137.5
TMLPS4	1500	$432 \times 649 \times 288$	147.2
TMLPS5	1900	$480 \times 721 \times 320$	153.9

a mean velocity difference (ΔU), an initial vorticity thickness ($\delta_{\omega,0} = \Delta U/(\partial\bar{u}/\partial y)_{max}$) and mass concentration in the free stream ($Y_{i,0}$). Dimensionless groups in above equations are Reynolds number($Re_{\omega,0}$), Schmidt number (Sc) and non-dimensional reaction rate (Rc).

The initial mean velocity distribution was given by a hyperbolic tangent velocity profile: $u(y) = 0.5\tanh(2y)$. Three dimensional random perturbation which has the same turbulent intensity profile with the experimental results (Wygnanski and Fielder, 1970) and banded white noise $|k_i| < 21$ was superposed on the mean velocity (Tanahashi et al., 2001). As for the initial concentration profile of passive scalars are also assumed to be hyperbolic tangent one; $Y_A(y) = 0.5+0.5\tanh(2y)$, $Y_B(y) = 0.5-0.5\tanh(2y)$. Computational domain was selected to be $4\Lambda \times 6\Lambda \times 8/3\Lambda$, where Λ is the most unstable wave length for the initial mean velocity profile. All variables are expanded by Fourier series in streamwise (x) and spanwise (z) directions and by sine/cosine series in transverse (y) direction. The boundary condition is periodic in the streamwise and spanwise directions and free-slip in the transverse direction. In the spanwise direction, the size of the computational domain is selected due to the 3/2 instability of the two-dimensional roller (Pierrehumbert and Widnall, 1982). In the transverse direction, that is selected to be enough to avoid mirror vortex effects caused by the free slip boundary condition.

DNS were conducted up to $Re_{\omega,0} = 1900$, where $Re_{\omega,0}$ denotes Reynolds number based on the initial vorticity thickness and the mean velocity difference, and reaction rate is changed for $Rc = 0.0$, 1.0 and 10 by assuming a single step reaction: A + B = 2P. To investigate Schmidt number effect, DNS are conducted for $Sc = 0.6$, 3.0 and 6.0 for $Re_{\omega,0} = 500$. The largest DNS are performed in 480 × 721 × 320 grid points. Aliasing errors from nonlinear terms in the governing equations are fully removed by 3/2 rule and time integration is conducted by the low-storage version of 3rd order Runge-Kutta scheme. Computations were carried out until after the saturation of the subharmonic mode ($t = 150$) for all cases.

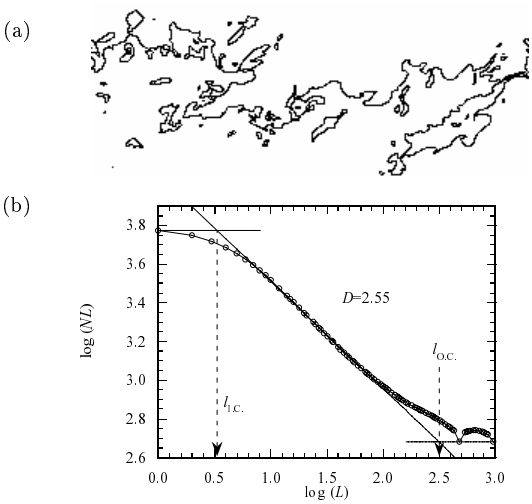

Figure 2: Contour lines of mass fraction of ($Y = 0.5$) on a typical $x-y$ plane (a) and $NL-L$ plots for 0.5 contour line of passive scalar on $x-y$ planes (b) for $Re_{\omega,0} = 1900$.

FRACTAL GEOMETRY OF SCALAR SURFACES

Mixing Transition

In Table 1, DNSs of non-reactive scalar are summarized. Schmidt number of these DNS is 0.6 and the maximum Reynolds number based Taylor microscale is 153.9 in fully-developed turbulent state ($t = 150$) at the center of shear layer. Figure 1 shows distribution of mass fraction on a $x-y$ plane in fully-developed turbulent state at $t = 150$. With the increase of Reynolds number, the distribution of mass fraction become complex and the mixing transition seems to occur between $Re_{\omega,0} = 500$ and $Re_{\omega,0} = 1300$. To investigate characteristics of the scalar mixing quantitatively, fractal analyses are introduced. As for contour lines on two-dimensional cross sections or contour surfaces of scalar, a two-dimensional (2D) or three-dimensional (3D) box counting methods are applied. In the 2D box counting method, contour lines on each $x-y$ or $y-z$ plane such as in Fig. 2(a) are analyzed, and one fractal plot ($NL-L$ plot) is obtained by averaging counting results on all planes as shown in Fig. 2(b). Here, L is the measure and NL is length of contour lines. From the $NL-L$ plot, an inner cutoff ($l_{I.C.}$) and an outer cutoff ($l_{O.C.}$) can be defined clearly. From a slope of the $NL-L$ plot, fractal dimension (D) is estimated using an additive law. As a result, inner cutoff, outer cutoff and fractal dimension are determined at a given time. As for the 3D box counting method, a fractal plot is obtained directly. The accuracy of the box counting method has been shown by our previous study (Miyauchi et al., 1994).

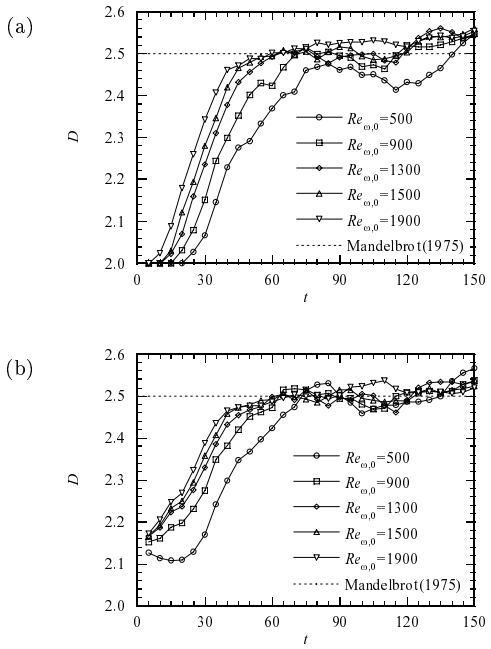

Figure 3: Developments of fractal dimension for non-reactive scalars(a) and Reynolds number dependence of the ratio of outer cutoff to inner cutoff(b).

Figure 3 shows temporal developments of the fractal dimension obtained from scalar distribution on $x-y$ and $y-z$ planes by a 2D box counting method. Both of fractal dimensions increase between t=30 and t=60. Higher Reynolds number case shows earlier increase of the fractal dimension. In this period, the turbulence transition of flow field occurs and lots of coherent fine scale structures are created (Tanahashi et al., 2001). In this transitional stage, the development of the fractal dimension reflects the transition process of velocity field and depends on the direction. In general, fractal dimensions of $x-y$ plane is lesser than those of $y-z$ planes. In the $x-y$ planes, roll-up of large scale organized structure (Kelvin-Helmholtz roller) induces scalar fluctuation and causes the increase of the fractal dimension. On the other hand, in the $y-z$ planes, streamwise vortices due to strong shear of the mean flow enhance the scalar mixing and increase the fractal dimension.

In the fully-developed turbulent state ($t > 60$), however, the directional dependence of the fractal dimension decreases. Furthermore, the fractal dimension in the fully-developed state does not depend on Reynolds number, and is about 2.5 even for the lowest Reynolds number case. This fractal dimension coincides with theoretical expectation by Mandelbrot (1975). In Fig. 4, fractal dimensions obtained from two-dimensional cross-section and three-dimensional surfaces are compared for $Re_{\omega,0} = 1900$. Fractal dimension from 3D surfaces coincides with that from $y-z$ planes in the transitional stage, and with that from $x-y$ planes in the fully-developed state. Hence, the additive law might be correct. The fractal dimension obtained from the present DNS is slightly larger than those by the experiments (Sreenivasan et al., 1989; Sreenivasan, 1991). In most of experiments, since fractal analyses have been conducted for concentration images including transitional region of the free shear flows, fractal dimension becomes to smaller value. The fact that fractal dimension in fully-developed state is independent to Reynolds number show that the mixing transition can not be characterized by the fractal dimension.

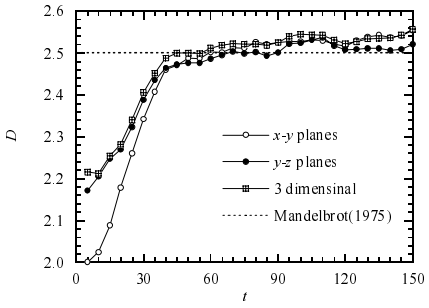

Figure 4: Comparison of fractal dimensions from two-dimensional cross-section and three-dimensional surfaces for $Re_{\omega,0} = 1900$.

Table 2: Inner and outer cutoffs of non-reactive scalar surfaces and their relations with the turbulence characteristic length scale.

$Re_{\omega,0}$	$l_{O.C.}$	$l_{I.C.}$	η	$l_{O.C.}/\Lambda$	$l_{I.C.}/\eta$
500	20.1	0.49	0.058	2.84	8.46
900	14.4	0.31	0.039	2.04	7.82
1300	14.1	0.24	0.029	2.00	8.18
1500	14.7	0.24	0.027	2.08	8.81
1900	18.5	0.20	0.022	2.60	8.89

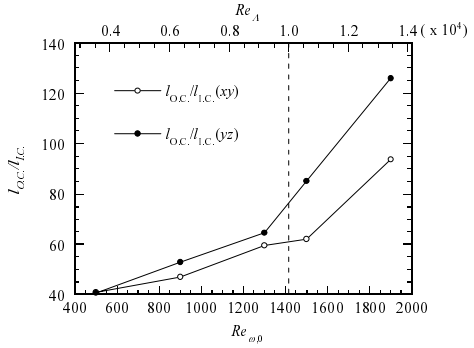

Figure 5: Reynolds number dependence of the ratio of outer cutoff to inner cutoff.

In Table 2, inner and outer cutoffs are compared with characteristic length scales of turbulent flow. The inner cutoff is about 8η for all cases and coincides with the most expected diameter of the coherent fine scale eddy (Tanahashi et al., 2001). The outer cutoff seems to be scaled by the large length scale which corresponds the size of the large scale coherent structure (Kelvin-Helmholtz roller). These results suggest that the inner cutoff also do not represent the mixing transition.

In Fig. 5, Reynolds number dependence of the ratio of the outer cutoff to the inner cutoff is shown for non-reactive scalars. The outer cutoff shows directional dependence even for fully-developed state. These ratios increase with the increase of Reynolds number nonlinearly. Dimotakis (2000) has reported that the mixing transition occurs if the Reynolds number based on the large scale (unstable wave length of shear layer, Λ), which is denoted as Re_Λ in this study, exceeds about 10^4. As shown in Fig. 5, $Re_\Lambda \approx 10^4$ corresponds to the drastic increase of difference between $l_{O.C.}$ and $l_{I.C.}$. Therefore, visual observations by human beings shows a phenomenological jump and this jump is defined as the mixing transition. In the theory of isotropic turbulence, scale separation between integral length (l_E) and

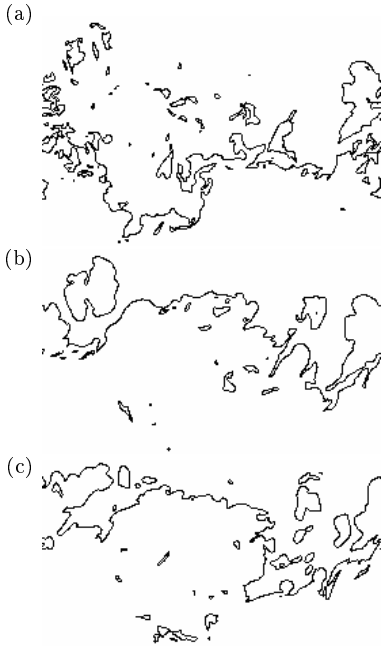

Figure 6: Contour lines of mass fraction ($Y_A = 0.5$) on a typical $x-y$ planes. (a):$Rc = 0.0$, (b):$Rc = 1.0$ and (c):$Rc = 10$ for $Re_{\omega,0} = 1500$ and $Sc = 0.6$.

Table 3: Numerical parameters for DNS of temporally-developing turbulent mixing layer with reactive scalar($Sc = 0.6$).

Run ID	$Re_{\omega,0}$	Rc	$N_x \times N_y \times N_z$
TMLRS1	500	1	$216 \times 325 \times 144$
TMLRS2	500	10	$216 \times 325 \times 144$
TMLRS3	900	1	$324 \times 487 \times 216$
TMLRS4	900	10	$324 \times 487 \times 216$
TMLRS5	1500	1	$432 \times 649 \times 288$
TMLRS6	1500	10	$432 \times 649 \times 288$

Kolmogorov length can be expressed as follows;

$$l/\eta \approx {Re_\lambda}^{3/4} \approx \frac{{Re_\lambda}^{3/2}}{15^{3/4}}. \quad (5)$$

If unstable wave length of shear layer was of the order of the integral length ($Re_l \approx Re_\Lambda$), the difference between $l_{O.C.}$ ($\approx l$) and $l_{I.C.}$ ($\approx 8\eta$) exceeds one decade at $Re_\lambda \approx 100$.

Effects of Chemical Reaction

Experimental observations in turbulent reactive flows (Gülder and Smallwood, 1995; Gülder et al., 2000) have suggested that fractal dimension of surfaces with chemical reaction such as flame is smaller than that of non-reactive surfaces (Sreenivasan et al., 1989; 1991). To investigate effects of chemical reaction on the fractal geometry, DNS of turbulent reacting mixing layer were conducted for different reaction rate and Reynolds number as listed in Table 3. Note that Δt for the temporal integration was carefully selected for high Rc cases.

Figure 6 shows contour lines of mass fraction ($Y_A = 0.5$) for different reaction rate cases in the fully-developed turbulent state. As for the reactive cases, distribution of mass fraction depend on Rc for small Rc (not shown here). However, for large Rc, distribution of mass fraction scarcely depend on Rc because the reaction is limited by the turbulent mixing. In Fig. 7, fractal dimension obtained by the 3D box counting method is shown for reactive cases. For comparison, fractal dimensions of non-reactive cases (Rc=0) are shown. For reactive cases, the increase of fractal dimension in the transitional stage delays significantly and the fractal dimension in the fully-developed state is smaller than that of non-reactive scalars. This is caused by the smoothing of the contour surfaces due to the consumption of reactant. Although the chemical reaction works to decrease of the fractal dimension, the decreasing rate is relatively small. In the fully-developed state, the fractal dimension keeps high values around $2.40 \sim 2.45$. These fractal dimensions seem to be asymptotic value for turbulent flows with diffusion-controlled reactions.

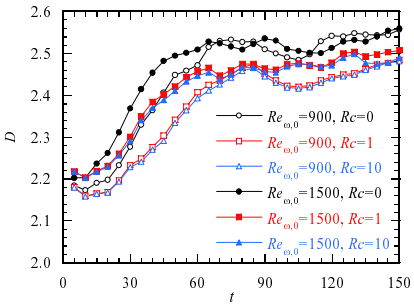

Figure 7: Developments of fractal dimension for reactive scalars.

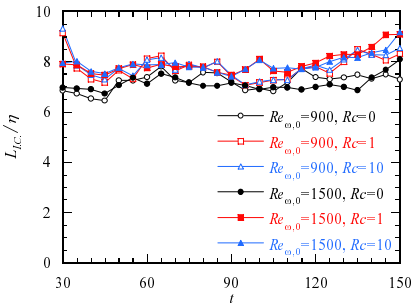

Figure 8: Development of ratio of the inner cutoff to Kolmogorov length scale for reactive scalars.

Table 4: Numerical parameters for DNS of temporally-developing turbulent mixing layer with passive scalar with high Sc ($Rc = 0$).

Run ID	$Re_{\omega,0}$	Sc	$N_x \times N_y \times N_z$
TMLPSH1	500	3.0	$480 \times 721 \times 320$
TMLPSH2	500	6.0	$480 \times 721 \times 320$

Figure 8 shows ratio of the inner cutoff to Kolmogorov length scale for reactive cases. The inner cutoff is about 8η in spite of reaction rate and Reynolds number, and coincides with those of non-reactive scalars. These results suggest that the coherent fine scale eddy dominates fine scale mixing in turbulence and controls local reaction rate for $Sc \approx 1$.

Effects of Schmidt Number

As for turbulent flows with transport of passive scalar with high Sc number, it is well-known that Batchelor length scale (η_B) becomes smaller than Kolmogorov length significantly because it is expressed by

$$\eta_B = \eta/Sc^{1/2}. \quad (6)$$

Numerical parameters for DNS with relatively high Sc are shown in Table 3. As the resolution of scalar fluctuation

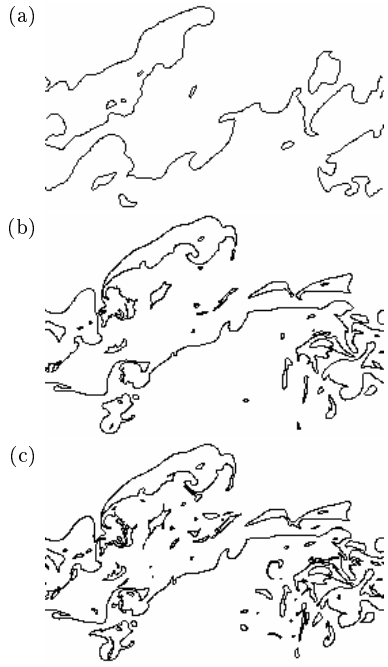

Figure 9: Contour lines of passive scalar ($Y_A = 0.5$) on a typical $x-y$ planes. (a):$Sc = 0.6$, (b):$Sc = 3.0$ and (c):$Sc = 6.0$ for $Re_{\omega,0} = 500$ and $Rc = 0$.

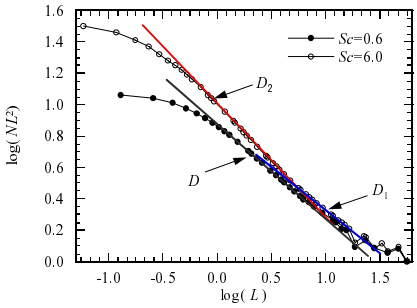

Figure 10: $NL - L$ plots for $Sc = 0.6$ and $Sc = 6.0$.

is more severe for high Sc, number of computational grids increases to $N_x \times N_y \times N_z = 480 \times 721 \times 320$.

Contour lines of passive scalar ($Y_A = 0.5$) on a $x-y$ plane are shown for different Sc cases in Fig. 9. Distribution of mass fraction becomes more complex for high Sc. Therefore, contour lines of scalar include small scale wrinkling. It should be noted that global pattern is similar even for different Sc because the turbulence structure is exactly same for these cases. The complexity of the contour lines is caused by local engulfment of scalar due to fine scale motion of turbulence. Figure 10 shows fractal plots($NL - L$ plots) for $Sc = 0.6$ and $Sc = 6.0$. As shown in above, only one fractal dimension (D) can be defined for moderate Sc, which represents the inertial subrange of turbulent velocity fluctuation and self-affinity of scalar surfaces. On the other hand, for high Sc number cases, two fractal dimensions (D_1 and D_2 in Fig. 10) can be defined. The first fractal dimension D_1 can be observed in relatively large scales and coincides with that of moderate Sc number case (D). The second fractal dimension D_2 can be defined in small scales and shows larger values around 2.7 and denotes self-similarity of scalar surfaces smaller than the Kolmogorov length. Temporal developments of these fractal dimensions are shown in Fig. 11. Compared with the low Sc case, the first fractal dimension is always small and the second one does large. However, difference between $Sc = 3.0$ and $Sc = 6.0$ is not significant. This result suggests that an asymptotic fractal dimension may exist for higher Sc. As discussed in above, the observation that the contour lines for $Sc = 6.0$ is more complex than that for $Sc = 3.0$ is mainly caused by the scale separation between η and η_B.

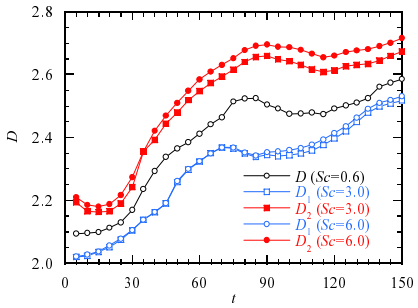

Figure 11: Development of fractal dimension of passive scalar with high Sc.

Table 5: Inner cutoff of the second fractal and its relation to dissipation length scales of velocity and scalar fluctuations

Sc	η	η_B	η_B/η	$l_{I.C.}/\eta_B$
0.6	0.0577	0.0745	1.29	6.2958
3.0	0.0577	0.0333	0.58	7.4119
6.0	0.0577	0.0235	0.41	8.4105

In Table 5, inner cutoff of the second fractal is compared with dissipation length scales of velocity and scalar fluctuations. As is expected theoretically, Batchelor length scale becomes smaller than Kolmogorov length scale. The inner cutoff of the second fractal is scaled by the Batchelor length scale and reaches to about $8\eta_B$. The self-similar fractal in small scales is induced by fine scale stirring of scalar by the coherent fine scale eddy of turbulence.

CONCLUSIONS

In this study, direct numerical simulations (DNSs) of turbulent mixing layer with non-reactive and reactive scalar transports have been conducted to investigate the mixing transition mechanism. DNS of non-reactive scalar up to $Re_{\omega,0} = 1900$ with moderate Schmidt number (Sc) show that fractal dimension of scalar surfaces in the fully-developed turbulent state is independent to Reynolds number and coincide with the theoretical expectation of Mandelbrot (1975) (≈ 2.5). The inner cutoff is 8 times Kolmogorov length and agrees with the most expected diameter of coherent fine scale eddy in turbulence. The mixing transition is characterized by the drastic increase of difference between the outer and inner cutoffs which occurs at $Re_\lambda \approx 100$. Due to this drastic increase, the observation of human beings gives a phenomenological jump. The directional dependence of the fractal dimension obtained from two-dimensional cross sections implies a possibility that the fractal dimension might be estimated incorrectly in the experiments.

DNS of reactive scalars show that the fractal dimension decreases to $2.40 \sim 2.45$ due to the chemical reaction, and that these fractal dimension are an asymptotic value for reactive scalar with fast chemistry. The fact that the inner cutoff for the reactive cases coincides with that of non-reactive cases shows that the coherent fine scale structure of turbulence dominates the mixing and reaction in small scales.

To investigate Schmidt number effects, DNS of non-

reactive scalar up to $Sc = 6.0$ has been conducted for moderate Reynolds number. For high Sc, two fractal dimensions can be defined. The first fractal dimension coincides with that of moderate Sc, whereas the second one shows larger values around 2.7. The inner cutoff of the second fractal reaches to about 8 times of Batchelor length scale for high Sc.

ACKNOWLEDGEMENT

This work is partially supported by Grant-in-Aid for Scientific Research (A)(No. 15206023) and (S)(No. 18106004) of Japan Society for the Promotion of Science and by Grant-in-Aid for Young Scientists (A)(No. 16686011) of the Ministry of Education, Culture, Sports, Science and Technology, Japan.

REFERENCES

Dimotakis, P., 2000, "The Mixing Transition in Turbulent Flows", *Journal of Fluid Mechanics*, Vol. 409, pp. 69-98.

Gouldin, F. C., Bray, K. N. C., and Chen, J. -Y., 1989, "Chemical Closure Model for Fractal Flamelets", *Combustion and Flame*, Vol. 77, pp. 241-259.

Gouldin, F. C., 1987, "An Application of Fractals to Modeling Premixed Turbulent Flames", *Combustion and Flame*, Vol. 68, pp. 249-266.

Gülder, Ö. L., 1990, "Turbulent Premixed Combustion Modelling Using Fractal Geometry", *Proceedings of Combustion Institute*, Vol. 23, pp. 835-842.

Gülder, Ö. L., Smallwood, G. J., 1995, "Inner Cutoff Scale of Flame Surface Wrinkling in Turbulent Premixed Flames ", *Combustion and Flame*, Vol. 103, pp. 107-114.

Gülder, Ö. L., Smallwood, G. J., Wong, R., Snelling, D. R., Smith, R., Deschamps, B. M., and Sautet, J. -C., 2000, "Flame Front Surface Characteristics in Turbulent Premixed Propane/Air Combustion", *Combustion and Flame*, Vol. 120, pp. 407-416.

Konrad, J. H., 1974, "An Experimental Investigation of Mixing in Two-Dimensional Turbulent Shear Flow with Applications to Diffusion-Limited Chemical Reactions", International Report, CIT-8-PU, Calif. Inst. Technol. Pasadena, CA.

Mandelbrot, B. B., 1975, "On the Geometry of Homogeneous Turbulence, with Stress on the Fractal Dimension of the Iso-Surfaces of Scalars", *Journal of Fluid Mechanics*, Vol. 72, pp. 401-416.

Miyauchi, T., Tanahashi M., and Gao, F., 1994, "Fractal Characteristics of Turbulent Diffusion Flames", *Combustion Science and Technology*, Vol. 96, pp. 135-154.

Peters, N., 1986, "Laminar Flamelet Concepts in Turbulent Combustion ", *Proceedings of Combustion Institute*, Vol. 21 pp. 1231-1250.

Pierrehumbert, R. T., and Widnall, S. E., 1982, "The Two- and Three- Dimensional Instabilities of a Spatially Periodic Shear Layer", *Journal of Fluid Mechanics*, Vol. 114, pp. 59-82.

Poinsot, T., Veynante, D., and Candel, S., 1990, "Diagrams of Premixed Turbulent Combustion Based on Direct Simulation", *Proceedings of Combustion Institute*, Vol. 23 pp. 613-619.

Smallwood, G. J., Gülder, Ö. L., Snelling, D. R., Deschamps, B. M., and Gökalp, I., 1995, "Characterization of Flame Front Surfaces in Turbulent Premixed Methane/Air Combustion", *Combustion and Flame*, Vol. 101, pp. 461-470.

Sreenivasan, K. R., Ramshankar, R., and Meneveau, C., 1989, "Mixing, Entrainment and Fractal Dimension of Surfaces in Turbulent Flows", *Proceedings of the Royal Society of London. Series A, Mathematical and Physical Sciences*, Vol. 421, pp. 79-108.

Sreenivasan, K. R., 1991, "Fractals and Multifractals in Fluid Turbulence", *Annual Review of Fluid Mechanics*, Vol. 23, pp. 539-600.

Tanahashi, M., Miyauchi, T., and Ikeda, J., 1997, "Identification of Coherent Fine Scale Structure in Turbulence", *Proceedings of the IUTAM Symposium. Simulation and Identification of Organized Structures in Flows*, pp. 131-140.

Tanahashi, M., Iwase, S., and Miyauchi, T., 2001, "Appearance and Alignment with Strain Rate of Coherent Fine Scale Eddies in Turbulent Mixing Layer", *Journal of Turbulence*, Vol. 2, p. 6.

Tanahashi, M., Kang, S.-J., Miyamoto, T., Shiokawa, S., and Miyauchi, T., 2004, "Scaling Law of Fine Scale Eddies in Turbulent Channel Flows up to $Re_\tau = 800$", *International Journal of Heat and Fluid Flow*, Vol. 25 pp. 331-340.

Yoshida, A., Kasahara, M., Tsuji, H., and Yanagisawa, T., 1994, "Fractal geometry application in estimation of turbulent burning velocity of wrinkled laminar flame", *Combustion Science and Technology*, Vol. 103, pp. 207-218.

Wygnanski, I., and Fielder, H. E., 1970, "The Two-Dimensional Mixing Region", *Journal of Fluid Mechanics*, Vol. 41, pp. 327-361.